Journal of
Ship&Ocean
Technology
©MARCH 2003

SOTECH Vol. 7, No. 1, pp. 1~12, 2003

Experimental Investigation on the Ultimate and Post-Ultimate Strength of Stiffened Plates under Axial Compression

Sang-Rai Cho[1] and Ick-Cho Song[2]

[1]School of Transportation Systems Engineering, University of Ulsan, Nam-Ulsan P.O. Box 18, Ulsan, 680-749, KOREA; E-mail: srcho@uou.ulsan.ac.kr
[2]The University of Ulsan, presently INP Heavy Industries

Abstract

Stiffened plates are among the most popular structural elements for marine structures like ships or offshore platforms. Many researchers have performed and reported the results of structural tests on stiffened plates in the open literature. However, the behaviour of stiffened plates in post-ultimate regime has not been fully reported. This paper reports the results of twenty-one axial compression tests including the initial imperfections and material properties of the test models. In aiming to investigate the post-ultimate behaviour of stiffened panels, the axial shortenings were increased up to far beyond the ultimate state. The results obtained from these tests can be utilised in substantiating design formulae in predicting the post-ultimate behaviour of stiffened plates.

Keywords: stiffened plates, experiment, axial compression, ultimate strength, post-ultimate behaviour

1 Introduction

Stiffened plates are extensively used as major structural elements of various onshore and offshore structures. For redundant structural systems composed of stiffened plates, like the ship's hull girder or bridge's box girder, some local elements of these structures may show post-ultimate behaviour before reaching the ultimate state of the whole system. However, most of the theoretical and experimental investigations on stiffened panels reported in the open literature so far mainly concern the responses up to, but not beyond, their ultimate states.

In order to efficiently analyse the structural behaviour of redundant stiffened plate structures it is necessary to provide the stress-strain relationship of stiffened plates(Smith 1977, Ostapenko 1981, Ueda et al 1984, Rutherford and Caldwell 1990, Yao and Nikolov1991, Gordo et al 1996). Smith (1977) obtained the relationship using the finite element analysis method for plates and then for beam-columns. Ueda et al (1984) obtained the relationships using the idealized structural unit method and other researchers proposed analytical ones. However, the relationship, especially in a post-ultimate regime, has not been fully substantiated with test results. In aiming to provide the experimental stress-strain relationship of stiffened plates subjected to combined axial compression

and end bending moment, twenty-one axial compression tests have been conducted and reported herein.

Slenderness parameters of the test models were chosen based upon those of typical ship structures. All models were fabricated by CO_2 gas welding. Before the main tests, the initial imperfections and material properties of test models were carefully measured. In the axial compression tests axial shortening and lateral deflection of each model were measured at every loading step. In aiming to investigate the post-ultimate behaviour of stiffened panels the axial shortenings were increased beyond the ultimate state.

The test results have been compared with the predictions by a recently derived strength formulation (Cho 2000). The comparisons show satisfactory agreements. However, for the test models having flat bar stiffeners whose slenderness for torsional buckling became larger, the formulation overestimates the ultimate strength. For the models, which failed due to stiffener tripping, the formulation also overestimates the resistance in the post-ultimate regime. In these experiments the effects of the free edge widths of stiffened plate models on their ultimate strength were also investigated. From this investigation it can be concluded that wider free edges can cause premature failure by the amplification of initial plate deformations.

2 Test models

For the axial compression tests, twenty-one models were fabricated. The nominal thickness of the plate was chosen to be 2 mm for all the models. Other dimensions for the ranges of model parameters were determined to fall into those of typical stiffened plates found on ships.

First, the plate and stiffeners were spot-welded and 10 mm thick end plates were attached. Then, the plate and stiffeners were fully welded and a round bar 25 mm in diameter was welded on to each end plate, hoping to simulate simply supported end conditions (see Figure 1).

The yield stress was determined to be 0.2 % proof stress. The average values of five tensile

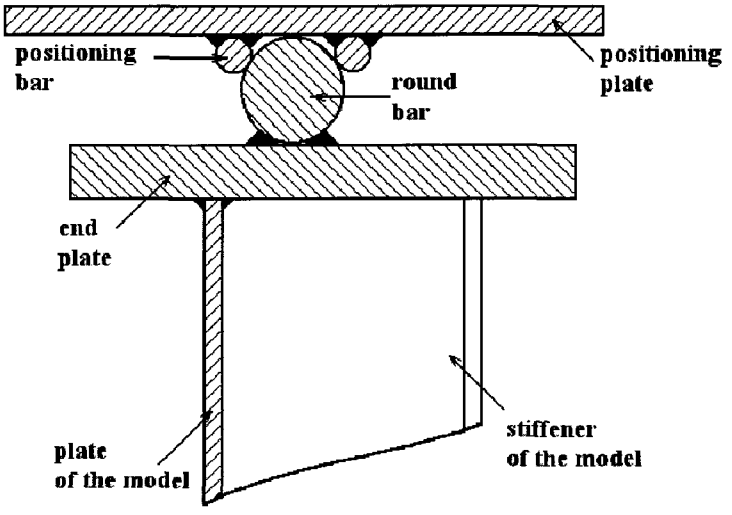

Figure 1: Arrangement of model ends to simulate simply supported boundaries

testing coupons from each parent sheet are representative of their material properties. After fabricating the models, grids were marked. The initial lateral deflections of plates and stiffeners and transverse distortion of stiffeners were carefully measured using dial gauges. The dimensions and material properties of the models are summarised in Table 1.

In the names of models the first figure after S indicates the number of stiffeners and the alphabets F and A after that figure represents flat bar stiffener and inverted angle stiffener respectively. Dimensions of plate and stiffener, number of stiffeners, initial imperfections, yield stress and Young's moduli of the models are included in the table. The material properties in the table are the average values of those of plate and stiffeners. As may be expected, the non-dimensionalised shape imperfections on the models are larger than those found on actual structures. In Figure 2, the initial shape of models S5F1 and S5A11 are visualised but the imperfections are amplified. As can be seen in the figure, the imperfections on the free edges are larger than those in the middle.

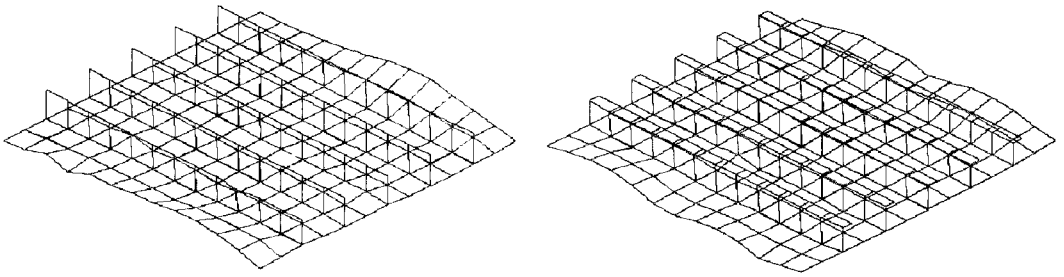

(a) Model S5F1 (b) Model S5A11

Figure 2: Initial shape of models

3 Axial compression tests

Axial compression tests were performed on twenty-one single-bay stiffened plates using a 100ton capacity universal testing machine. The main purpose of the tests was to provide not only the experimental results of the ultimate state but far beyond the ultimate state. The effects of the free edge width of the test models on the ultimate strength of stiffened plates were also investigated in the tests. The locations of end round bars were measured to be the distances from the opposite plate surface to the stiffeners. From the locations of the round bars, the eccentricities of applied axial compression can be estimated.

Axial compressive load was applied incrementally in the tests. In the post-ultimate regime, however, the testing machine was controlled by displacement. In the tests the axial shortening, lateral deflections of plate and transverse deflections of stiffener were measured by LVDTs at every loading step. The results of the axial compression tests are given in Table 2 together with eccentricity of applied load, e, and slenderness parameters, β, λ_c and λ_t whose definitions are given as follows :

Table 1: Geometry and material properties of test models

Model	Dimension				No. of Stiff	Initial imperfection			σ_Y $[E]$ (N/mm^2)
	B* [b] (mm)	l** (mm)	t** (mm)	Stiffener (mm)		Plate+ (w_i/t)	Stiffener		
							Trans++ (w_{ti}/l)	Lateral+ (w_{li}/l)	
S3F11	400 [100]	600	2.13	50×2.13F.B	3	-0.85	-0.00158	0.00158	332.4 [248200]
S3F12	400 [100]	600	2.13	50×2.13F.B	3	-1.40	0.00225	0.00342	332.4 [248200]
S3F2	300 [100]	600	2.13	50×2.13F.B	3	1.35	0.00167	0.00308	332.4 [248200]
S3F3	250 [100]	600	2.13	50×2.13F.B	3	0.65	-0.00092	0.00225	332.4 [248200]
S5F1	600 [100]	600	2.13	50×2.13F.B	5	-0.70	0.00333	0.00208	332.4 [248200]
S5F2	500 [100]	600	2.13	50×2.13F.B	5	-1.05	-0.00208	0.00308	332.4 [248200]
S5F3	450 [100]	600	2.13	50×2.13F.B	5	-1.50	-0.00208	0.00475	332.4 [248200]
S3A1	400 [100]	600	2.13	40×15×2.13I.A	3	-0.40	0.00125	0.00125	329.7 [234800]
S3A2	300 [100]	600	2.13	40×15×2.13I.A	3	-0.75	0.00042	0.00292	329.7 [234800]
S3A3	250 [100]	600	2.13	40×15×2.13I.A	3	-1.00	-0.00083	0.00217	329.7 [234800]
S5A11	600 [100]	600	2.13	40×15×2.13I.A	5	0.90	-0.00250	-0.00300	329.7 [234800]
S5A2	500 [100]	600	2.13	40×15×2.13I.A	5	-0.90	0.00125	-0.00333	329.7 [234800]
S5A3	450 [100]	600	2.13	40×15×2.13I.A	5	-0.85	-0.00125	0.00208	329.7 [234800]
S3F100	260 [100]	600	1.86	50×1.99F.B	3	0.93	-0.00250	-0.00403	316.4 [220300]
S3A100	260 [100]	600	1.86	40×15×1.99I.A	3	0.47	0.00250	0.00520	316.0 [220200]
S5A12	600 [100]	600	1.86	40×15×1.99I.A	5	1.46	0.00330	0.01120	317.1 [220700]
S3F80	220 [80]	700	1.86	40×1.99F.B	3	-1.75	0.00210	0.00550	316.5 [220400]
S3F120	300 [120]	700	1.86	60×1.99F.B	3	0.85	0.00360	-0.00200	316.2 [220300]
S5F80	380 [80]	700	1.86	60×1.99F.B	5	2.25	0.00290	-0.00613	315.3 [219800]
S3A80	220 [80]	700	1.86	50×10×1.99I.A	3	2.01	0.00140	0.00663	315.2 [219700]
S3A120	300 [120]	700	1.86	30×10×1.99I.A	3	1.51	-0.00210	0.00430	317.5 [220900]

Notes:

* B and b are the overall breadth and the stiffener spacing respectively

** l and t are the overall length and the thickness respectively

\+ the initial lateral imperfection of plate and stiffener ; (+) toward stiffener, (-) toward plate

++ the initial transverse imperfection of stiffener ; (+) toward left, (-) toward right

Table 2: Axial compression test results

Model	Parameter			e*	Collapse	Max.	σ_u	σ_u/σ_Y		
	β	λ_c	λ_t	(mm)	Mode**	Load(KN)	(N/mm^2)	test	pred+	Xm++
S3F11	1.72	0.47	1.36	-3.41	Mode II	171.7	146.6	0.441	0.598	0.737
S3F12	1.72	0.47	1.36	-4.42	Mode II	198.2	169.2	0.509	0.559	0.910
S3F2	1.72	0.47	1.36	-2.49	Mode II	183.4	191.4	0.576	0.667	0.864
S3F3	1.72	0.47	1.36	-1.62	Mode II	196.2	230.3	0.693	0.718	0.964
S5F1	1.72	0.47	1.36	-3.83	Mode II	259.0	143.1	0.431	0.587	0.733
S5F2	1.72	0.47	1.36	-2.71	Mode II	238.4	149.2	0.449	0.653	0.688
S5F3	1.72	0.47	1.36	-0.97	Mode II	316.9	212.5	0.639	0.743	0.860
S3A1	1.76	0.47	1.13	-4.13	Mode I	247.2	205.4	0.623	0.580	1.074
S3A2	1.76	0.47	1.13	-2.42	Mode I	241.3	243.7	0.739	0.676	1.093
S3A3	1.76	0.47	1.13	-0.76	Mode I	230.5	260.8	0.791	0.761	1.040
S5A11	1.76	0.47	1.13	-3.00	Mode II	409.1	219.5	0.666	0.632	1.053
S5A2	1.76	0.47	1.13	-2.00	Mode II	347.3	210.4	0.638	0.690	0.924
S5A3	1.76	0.47	1.13	-1.23	Mode I	331.6	214.7	0.651	0.732	0.890
S3F100	2.05	0.48	1.51	-2.50	Mode II	130.1	166.3	0.526	0.655	0.796
S3A100	2.06	0.47	1.20	-0.39	Mode I	210.7	259.5	0.821	0.751	1.091
S5A12	2.05	0.47	1.20	-3.58	Mode I	348.8	209.7	0.661	0.597	1.109
S3F80	1.64	0.70	1.22	12.18	Mode I	79.1	122.1	0.386	0.367	1.050
S3F120	2.47	0.47	1.80	-9.61	Mode II	78.1	85.2	0.269	0.480	0.560
S5F80	1.65	0.44	1.80	-9.59	Mode II	118.7	91.0	0.289	0.535	0.539
S3A80	1.65	0.45	1.58	-19.59	Mode II	88.5	115.3	0.366	0.390	0.937
S3A120	2.46	0.83	1.04	11.19	Mode I	82.6	103.7	0.327	0.327	0.998

Notes:

* e is the distance of applied load location from the elastic neutral axis of the stiffened plate

** failure mode I and II are those of plate induced and stiffener induced respectively

\+ the predicted ultimate strengths were obtained using equation (1)

++ Xm is the ratio of actual to predicted ultimate strength

β is the plate slenderness, $(b/t)\sqrt{\sigma_Y/E}$

λ_c is the slenderness of the stiffener for column buckling, $\sqrt{\sigma_Y/\sigma_{ec}}$

λ_t is the slenderness of the stiffener for torsional buckling, $\sqrt{\sigma_Y/\sigma_{et}}$

where

b is the longitudinal stiffener spacing

t is the thickness of the plate

σ_Y, E are the yield stress and Young's modulus of the material respectively

σ_{ec} is the Euler column buckling stress of stiffener including the associate plate

σ_{et} is the elastic torsional buckling stress of stiffener, $\frac{1}{I_o}(GJ + \frac{4\pi^2}{L^2}EC_w)$

$I_o = I_w + A_s e_s^2 + I_f$, polar moment of inertia of the stiffener

I_w is the polar moment of inertia of stiffener web

I_f is the polar moment of inertia of stiffener flange

e_s is the distance between the stiffener centroid (plate excluded) and its toe

$J_x = (h_{sw}t_{sw}^3 + h_{sf}t_{sf}^3)/3$, St. Venant torsion constant of longitudinal stiffener

h_{sw}, t_{sw} are the width and thickness of the web of longitudinal stiffener respectively

h_{sf}, t_{sf} are the width and thickness of the flange of longitudinal stiffener respectively

$C_w \approx I_f(\frac{h_w+t_f}{2})^2$, torsional warping constant of longitudinal stiffener

The photographs of collapsed models, models S3A3 and S5A2, are presented in Figure 3. It is shown that the former failed due to plate buckling while the latter failed on account of the coupling mode of column and torsional bucklings.

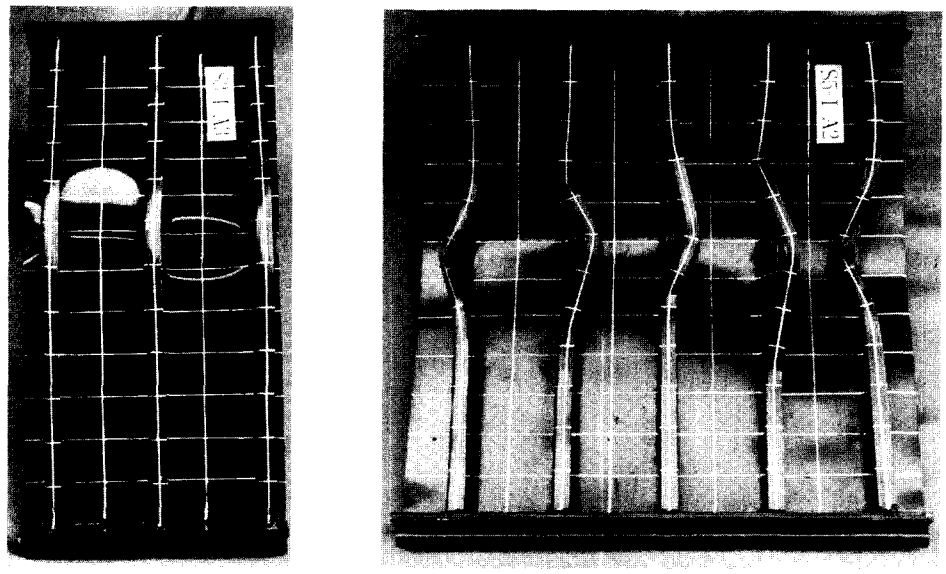

(a) Model S3A3 (b) Model S5A2

Figure 3: Collapsed models after axial compression test

4 Discussion

4.1 Ultimate strength

For the prediction of the ultimate strength of multi-bay stiffened plates under combined axial compression, lateral pressure and end bending moment, a robust formulation had been derived (Cho 2000). The formulation put forth by this paper was based on the generalised Merchant-Rankine formula to consider all possible failure modes and their interactions. The knock-down factors in the equation were obtained from the regression analysis of the test results of multi-bay stiffened

plate models. The detail procedures to derive this design equation can be found elsewhere (Cho 2000). The design formulation used for the prediction is given as (1) as follows:

$$\left(\frac{\sigma_{ao}}{\rho_c\sigma_{ec}} + \frac{\sigma_{ao}+\sigma_{bso}}{\rho_t\sigma_{et}} + \frac{\sigma_{ao}}{\rho_{oa}\sigma_{eo}}\right)^2 + \left(\frac{\sigma_a+\sigma_b}{\sigma_Y}\right)^2 = 1 \tag{1}$$

where

σ_a is the applied axial stress

$\sigma_{ao} = \sigma_a$ for $\sigma_a < 0$, $\sigma_{ao} = 0$ for $\sigma_a > 0$

$\sigma_{bso} = \sigma_{bs}$ for $\sigma_{bs} < 0$, $\sigma_{bso} = 0$ for $\sigma_{bs} > 0$

σ_{bs} is the bending stress at stiffener flange due to M_{eq},

$\sigma_b = \sigma_Y \frac{M_{eq}}{M_p}$, equivalent bending stress due to end bending moment and lateral pressure

$M_{eq} = M_e + \frac{pbl^2}{16}$

M_e is the applied end bending moment

p is the applied lateral pressure

l is the transverse stiffener spacing

$\sigma_Y = (\sigma_{Yp}A_p + \sigma_{Ys}A_s)/A_{ps}$, mean yield stress

$\sigma_{eo} = \frac{n^2\pi^2 D_y}{a_x B^2}\left(\frac{D_x B^2}{D_y L^2} + \frac{2m^2 D_{xy}}{n^2 D_y} + \frac{m^4 L^2}{n^4 B^2}\right)$, overall grillage buckling stress

L, B are overall length and breadth of the stiffened plate

a_x is the average cross-sectional area per unit width of plating and longitudinal stiffeners

$D_x = Ei_x/b$, effective longitudinal flexural rigidity per unit width

i_x is the moment of inertia of a longitudinal stiffener including the associate plating

$D_y = Ei_y/l$, effective transverse flexural rigidity per unit width

i_y is the moment of inertia of a transverse stiffener including the associate plating

$D_{xy} = a_x\{\frac{Et^3}{12(1-v^2)} + \frac{G}{2}(\frac{J_x}{b} + \frac{J_y}{l})\}$, twisting rigidity per unit width

v, G are the Poisson's ratio and shear modulus of the material respectively

$J_y = (h_{tsf}t_{tf}^3 + h_{tw}t_{tw}^3)/3$, St. Venant torsion constant of transverse stiffener

h_{tw}, t_{tw} are the width and thickness of the web of transverse stiffener respectively

h_{tf}, t_{tf} are the width and thickness of the flange of transverse stiffener respectively

$\rho_c = 2.46\beta^{-0.9}\lambda_c^{1.9}\lambda_t^{-0.2}$, knock-down factor for column buckling of stiffener

$\rho_t = 0.75\beta^{1.7}\lambda_c^{-1.9}\lambda_t^{3.4}$, knock-down factor for torsional buckling of stiffener

$\rho_{oa} = 1.0$, knock-down factor for overall grillage buckling

As mention earlier the predicted ultimate strength for the test models using (1) are given in Table 2. The ratios of actual to predicted strength yield mean and COV of 0.901 and 19.0 % for twenty-one test models. However, there are big discrepancies between the models of flat bar stiffeners and those having inverted angle ones. For eleven models having flat bar stiffeners mean and COV are 0.791 and 20.2 % respectively. But for ten models having inverted angle stiffeners these values are improved a lot to 1.020 and 7.74 %. This will be discussed further later.

4.2 Effects of free edge width

When designing stiffened plate test models subjected to axial compression, it is necessary to determine the width of free edges along the unloaded sides. As mentioned earlier, in order to investigate the effects of the width of free edges on their ultimate strengths, four groups of nominally identical models but having deferent widths of free edges were fabricated. Group FB1 consists of models S3F11, S3F12, S3F2 and S3F3, which are nominally identical but their widths of free edges are 100 mm, 100 mm, 50 mm and 25 mm respectively. Group FB2 consists of models S5F1, S5F2 and S5F3, whose free edge widths are 100 mm, 50 mm and 25 mm respectively. These two groups are of flat bar stiffeners. Groups IA1 and IA2 consist of models S3A1, S3A2 and S3A3 and S5A11, S5A2 and S5A3 respectively. These two groups are of inverted angle stiffeners.

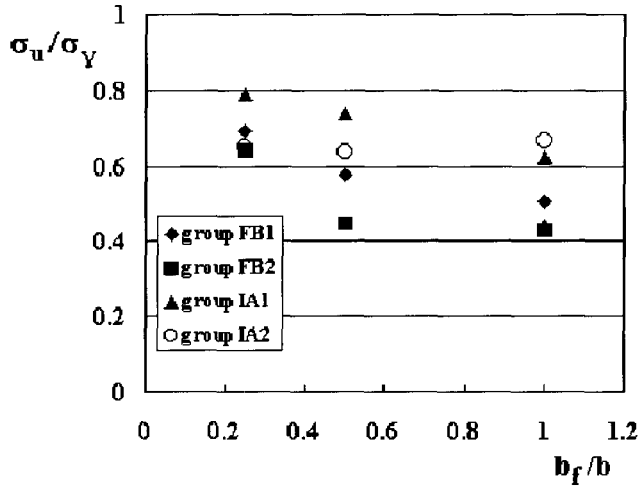

Figure 4: Effect of the free edge width on the ultimate strength of stiffened plates

In Figure 4, the non-dimensionalised ultimate strengths by yield stress are plotted against the ratios of free edge widths to stiffener spacing. As can be seen in the figure the ultimate strengths

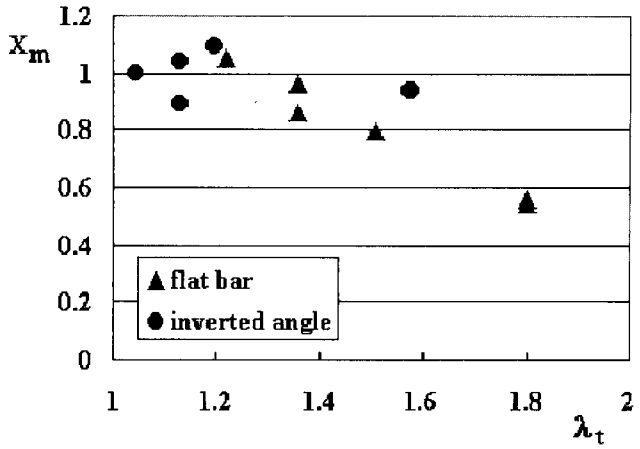

Figure 5: Skewness of predictions using equation (1) depending on the tripping slenderness ratio λ_t

are apparently reduced when increasing the width of free edge. This tendency is very strong for groups FB1, FB2 and IA1. But for group IA2 the tendency is not apparent. This can be explained that wider free edges, which have larger initial shape imperfection, can cause premature failure by the amplification of initial plate deformations. Based upon the results of this investigation it can be recommendable that the widths of free edge of models need to be less than around 30 % of the stiffener spacings to avoid premature failure.

4.3 Skewness of the ultimate strength formulation

As briefly discussed in sec. 4.1, the predictions using (1) provide different levels of accuracy for inverted angle stiffener models and those of flat bar stiffeners. In Figure 5, for the models whose free edge widths are smaller than 40 % of their stiffener spacing the ratios of actual to predicted strength are plotted against λ_t, slenderness of stiffener for torsional buckling. It can be clearly seen that for the models of flat bar stiffeners the formulation overestimates the strengths when λ_t becomes large. But for the models having inverted angle stiffeners quite accurate predictions can be provided regardless of λ_t values. This may indicate that a recourse to revising the knock-down factors can improve the accuracy and reliability of the predictions by the strength formulation.

4.4 Post-ultimate behaviour

Predicting the post-ultimate behaviour of stiffened plates is necessary for analysing the ultimate strength of redundant structures. An attempt has been made herein to provide an approximation of the average strain-average stress relation for stiffened plates. The relation is assumed:

(1) to be linear until the average stress is less than or equal to two thirds of the ultimate value,

(2) to be sinusoidal shape up to the ultimate value and

(3) for a plastic hinge to be formed at the mid-length of the stiffener in the post-ultimate regime.

This relation can be expressed as follows:

$$\frac{\sigma}{\sigma_Y} = \frac{\varepsilon}{\varepsilon_Y} \qquad for \qquad \frac{\varepsilon}{\varepsilon_Y} \leq \frac{\varepsilon_l}{\varepsilon_Y} \tag{2a}$$

$$\frac{\sigma}{\sigma_Y} = \frac{1}{3}\frac{\sigma_u}{\sigma_Y}[2 + sin(\frac{\pi}{2}\frac{\varepsilon - \varepsilon_l}{\varepsilon_u - \varepsilon_l})] \qquad for \qquad \frac{\varepsilon_l}{\varepsilon_Y} < \frac{\varepsilon}{\varepsilon_Y} < \frac{\varepsilon_u}{\varepsilon_Y} \tag{2b}$$

$$\frac{\sigma}{\sigma_Y} = \frac{\sigma_u}{\sigma_Y}\frac{\sqrt{\varepsilon_u(2-\varepsilon_u)} + 2\delta_i}{\sqrt{\varepsilon(2-\varepsilon)} + 2\delta_i} \qquad for \qquad \frac{\varepsilon}{\varepsilon_Y} > \frac{\varepsilon_u}{\varepsilon_Y} \tag{2c}$$

where

σ_u is the ultimate compressive stress, which can be obtained from (1)

$\frac{\varepsilon_l}{\varepsilon_Y} = \frac{2}{3}\frac{\sigma_u}{\sigma_Y}$

$\frac{\varepsilon_u}{\varepsilon_Y} = 0.06\beta^{2.8}\lambda_c^{-1.2}\lambda_t^{-1.2}(\frac{\sigma_u}{\sigma_Y})^{1.6}$

δ_i is the non-dimensionalised initial lateral imperfection of the stiffener

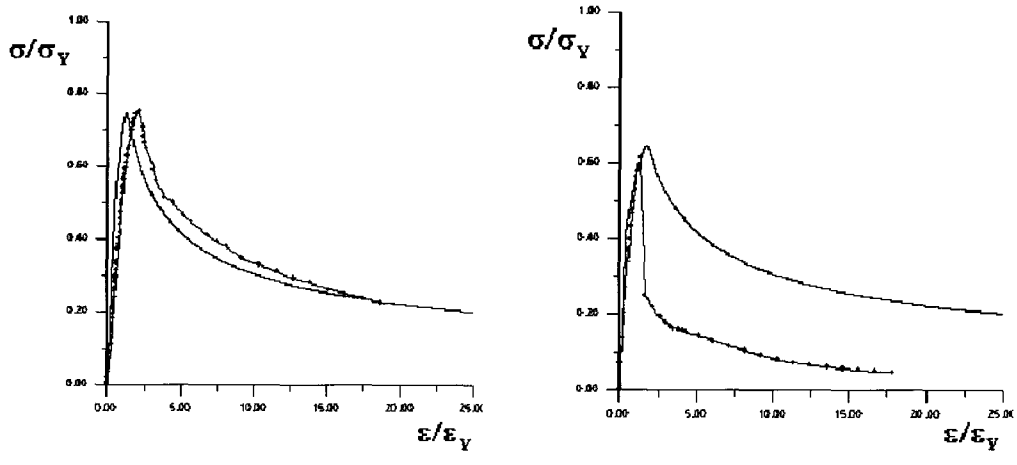

(a) Model S3A100 (b) Model S3F2

Figure 6: Comparison of the predicted average strain-stress relation for stiffened plates with test results (•: exp., —: pred.)

In Figure 6, the average stress-strain relations obtained from the test results of models S3A100 and S3F2 are shown together with those predicted by (2a $\sim$ c) and (1). For Model S3A100, which failed due to plate buckling, the predication agrees quite well with test results. But for Model S3F2, which failed due to coupling modes of column and torsional buckling of the stiffeners, show

a substantial deviation. The predictions overestimate quite much in the post-ultimate regime. It seems likely that further development of torsional deformation of the stiffeners in the region is attributable to the deviation. Therefore, to improve prediction, it is necessary to consider further stiffener deformation in the post-ultimate regime.

5 Conclusions

Twenty-one axial compression tests on stiffened plates have been successfully conducted and reported in this paper, which provide not only the structural response of stiffened plates up to the ultimate state but also that of post-ultimate regime.

The effects of free edge width on the ultimate strength have been investigated in this study. Based upon the results of this investigation it can be recommendable that the widths of free edge of test models need to be less than around 30 % of the stiffener spacings to avoid premature failure.

The predicted ultimate strength using the strngth formulation, (1) and the experimental values show very good agreement except for some of the models of flat bar stiffeners whose tripping slenderness parameters, λ_t, are large. Equations, (2a $\sim$ c) to trace the average stress - average strain relations have been proposed. They can then be conveniently utilised in the ultimate strength analysis of redundant structures composed of stiffened plates.

In order to improve the prediction of ultimate strengths it is necessary to modify the formulations especially for stiffened plates having flat bar stiffeners of large tripping slenderness parameter. For the more realistic representation of the structural behaviour in post-ultimate regime, further transverse deformation of flat bar stiffeners needs to consider in the formulation.

Acknowledgements

This work was financially supported by Korea Research Foundation Grant (KRF-1997- 001-E00124).

References

CHO, S.R. 2000 Ultimate strength formulation for ship's grillages under combined loadings. J. of Engineering Research, **31**, **2**, pp. 145-157

GORDO, J. M., GUARES SOARES, C. AND FAULKNER, D. 1996 Approximate assessment of the ultimate longitudinal strength of hull girder. J. of Ship Research, **40**, **1**, pp. 60-69

OSTAPENKO, A. 1981 Strength of ship hull girders under moment, shear and torque. Proc. of SSC -SNAME Extreme Loads Response Symp, Arlington, pp. 149-166

RUTHERFORD, S. E. AND CALDWELL, J. B. 1990 Ultimate longitudinal strength of ships: a case study. SNAME Trans, **98**, pp. 441-471

SMITH, C. 1977 Influence of local compression failure on ultimate longitudinal strength of a ship's hull. Proc. of 2nd Intl Symp. on Practical Design in Shipbuilding, PRADS '77, Tokyo & Seoul, pp. 73-79

UEDA, Y., RASHED, S. M. H. AND PAIK, J. K. 1984 Plate and stiffened plate units of the idealized structural unit method - under in-plane loading. J. of Society of Naval Architects of Japan, **156**, pp. 366-376

YAO, T. AND NIKOLOV, P. I. 1991 Progressive collapse analysis of a ship's hull under longi tudinal bending. J. of Society of Naval Architects of Japan, **170**, pp. 449-461